

UniV2D: Bridging Visual Restoration and Semantic Perception for Underwater Salient Object Detection

Laibin Chang¹, Shaodong Wang¹, Yunke Wang², Xu Zhang¹, Kui Jiang³, Chang Xu², Bo Du¹

¹ School of Computer Science, Wuhan University

² School of Computer Science, The University of Sydney

³ School of Computer Science and Technology, Harbin Institute of Technology

Abstract

Underwater salient object detection (USOD) plays a vital role in marine vision tasks but remains fundamentally challenging due to severe visual degradation, such as selective absorption and medium scattering. Conventional pipelines typically adopt a sequential "enhance-then-detect" paradigm. However, isolating low-level visual restoration from high-level semantic perception often leads to semantic inconsistency, where the restored images may not be optimal for detection and can even introduce task-irrelevant noise. To break this sequential bottleneck, we propose UniV2D, a Unified Vision-to-Detection Network that jointly optimizes visual restoration and salient object detection within a mutually beneficial framework. Unlike traditional methods that rely on disjointed pipelines or rigid physical priors, UniV2D introduces a semantic-driven learning paradigm: high-level saliency semantics actively guide the restoration process, while the restored visual cues reciprocally enhance saliency perception. Specifically, UniV2D features a hierarchical dual-branch architecture. It first employs a self-calibrated decoder to predict initial saliency masks alongside a mask-aware restoration module to reconstruct image content. Subsequently, a saliency-guided refinement module equipped with cross-level modulation is utilized to align structural fidelity with semantic consistency. Extensive experiments across multiple benchmarks demonstrate that UniV2D significantly outperforms state-of-the-art methods in both quantitative and qualitative evaluations, establishing a new standard for joint underwater perception.

1. Introduction

Salient Object Detection (SOD) [21, 67] aims to identify and segment the most visually prominent regions within an image, typically corresponding to foreground objects that attract human attention [12, 13, 15, 22, 28, 45, 65, 94]. Al-

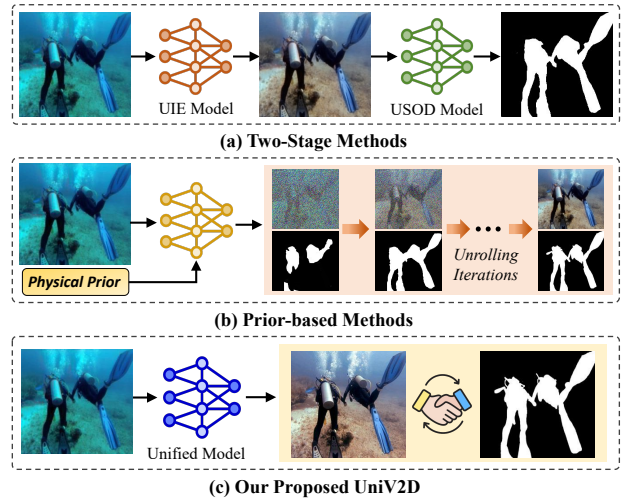


Figure 1. Comparison of different paradigms for joint Underwater Image Enhancement (UIE) and Salient Object Detection (USOD). (a) Two-stage methods decouple UIE and USOD into independent networks, resulting in limited cross-task synergy. (b) Prior-based methods (e.g., WaterDiffusion) require auxiliary physical priors and computationally expensive iterative sampling. (c) Our UniV2D establishes a unified framework for simultaneous UIE and USOD, achieving explicit task interaction and efficient one-shot inference.

though considerable progress has been achieved in terrestrial SOD tasks, largely facilitated by large-scale annotated datasets and advances in deep learning architectures, the performance of these models deteriorates markedly when applied to underwater environments [51, 75]. This decline primarily stems from the inherent challenges of underwater imaging, including light attenuation, color distortion, and low contrast, which collectively lead to the loss of texture and fine details [4, 40, 42, 83]. Such degradations severely weaken visual saliency cues, making it increasingly difficult for conventional models to accurately detect and localize salient objects in complex underwater scenes.

Underwater Salient Object Detection (USOD) has gar-

nered increasing attention due to its strategic importance in various vision-based marine exploration applications [25, 43, 44, 54, 88, 92]. Despite its potential, USOD faces several inherent challenges: 1) Poor visibility in underwater imagery impedes the accurate localization of salient regions [8, 26, 39]; 2) Underwater devices with limited computational resources are not suitable for deploying high-complexity models [7, 47, 69, 70]. To mitigate these issues, existing USOD methods [35, 49, 72, 73, 93] commonly incorporate handcrafted underwater imaging priors (such as transmission or depth maps) to compensate for visual artifacts. However, such heavy reliance on physical priors limits model generalization, as these priors are frequently unavailable or unreliable in diverse real-world conditions. Furthermore, while several sophisticated architectures [17, 27, 74] have pushed the boundaries of detection performance, they inevitably introduce excessive parameter counts and computational overhead, which significantly restricts their practical deployment on resource-constrained underwater devices.

To alleviate the interference caused by underwater degradation, a straightforward solution is to adopt a sequential "enhance-then-detect" pipeline, where a dedicated Underwater Image Enhancement (UIE) model pre-processes the image before salient object detection [9, 46], as illustrated in Fig. 1(a). However, most UIE methods prioritize global perceptual quality and may inadvertently overlook or even distort local saliency cues [86]. This two-stage paradigm fundamentally decouples low-level visual restoration from high-level semantic perception, lacking an effective mechanism for cross-task collaborative representation learning. While UIE aims to restore visual clarity and USOD requires structural fidelity for precise localization, these two objectives are often not perfectly aligned in disjointed frameworks. Recently, diffusion-based approaches like Water-Diffusion [5] have attempted to bridge this gap by jointly optimizing restoration and detection through iterative unrolling and physical imaging priors, as shown in Fig. 1(b). Although these methods achieve impressive results, their heavy reliance on handcrafted imaging assumptions and the high computational cost of multiple optimization iterations limit their practical efficiency. These limitations motivate us to develop a more efficient collaborative framework that seamlessly integrates visual restoration and salient object detection within a unified architecture.

Motivated by the above analysis, we propose UniV2D, a novel and unified framework designed to jointly optimize underwater image restoration and salient object detection in a mutually reinforcing manner. Diverging from the conventional sequential pipelines or those tethered to rigid physical priors, UniV2D introduces a semantic-driven dual-branch architecture that establishes explicit task interaction from the initial decoding stages. Specifically, the Self-Calibrated

Saliency Masking (SCSM) module progressively generates a saliency map by incorporating spatial reweighting with token-guided feature calibration. The Mask-Aware Content Restoration (MACR) module leverages this predicted saliency as structural guidance to reconstruct clear images with enhanced content consistency. These preliminary outputs are further refined through a saliency-guided cross-level refinement procedure, which employs Cross-Level Feature Modulation (CLFM) to facilitate bidirectional feature interaction across multiple scales. Owing to its streamlined design and efficient learning paradigm, UniV2D achieves robust performance on both tasks while maintaining a significantly low computational overhead.

Our key contributions are summarized as follows:

- We propose UniV2D, a unified and lightweight framework that jointly optimizes underwater image restoration and salient object detection without relying on handcrafted physical priors or iterative optimization.
- We design a coarse-to-refinement architecture featuring SCSM, MACR, and CLFM modules, which effectively bridges the gap between low-level visual restoration and high-level semantic perception via bidirectional feature interaction.
- Extensive experiments demonstrate that UniV2D outperforms existing state-of-the-art UIE and USOD solutions in both qualitative and quantitative outcomes.

2. Related Work

Underwater Image Enhancement. UIE is a practical yet challenging task within the field of visual restoration, which mainly includes the physics-based and deep learning-based methods [20, 48, 63, 66, 81, 82]. These physics-based methods [11] aim to improve visual perception by directly manipulating image pixel values with well-designed techniques, regardless of the underwater degradation mechanism, including multi-scale fusion [62, 79], Retinex-based [89, 96], and histogram equalization [29]. Deep learning-based UIE methods [3] concentrate on enhancing degraded images by autonomously learning non-linear restoration mappings from paired underwater image datasets [84, 95]. Recently, diffusion-based methods [2, 16] have been proposed for underwater image restoration, such as UW-DDPM [50], DiffUIE [59], WF-Diff [87], and DCGF [85]. Additionally, several domain adversarial learning networks have been developed to improve the adaptability of UIE models, including TUDA [68], Semi-Net [30], UICoE-Net [57], *etc.* While these methods demonstrate a certain level of domain adaptation, they do not explicitly prioritize the enhancement of salient regions. As a result, they remain inadequate for supporting downstream salient object detection tasks.

Underwater Salient Object Detection. Early feature-based USOD methods [36, 37] attempt to encode low-level

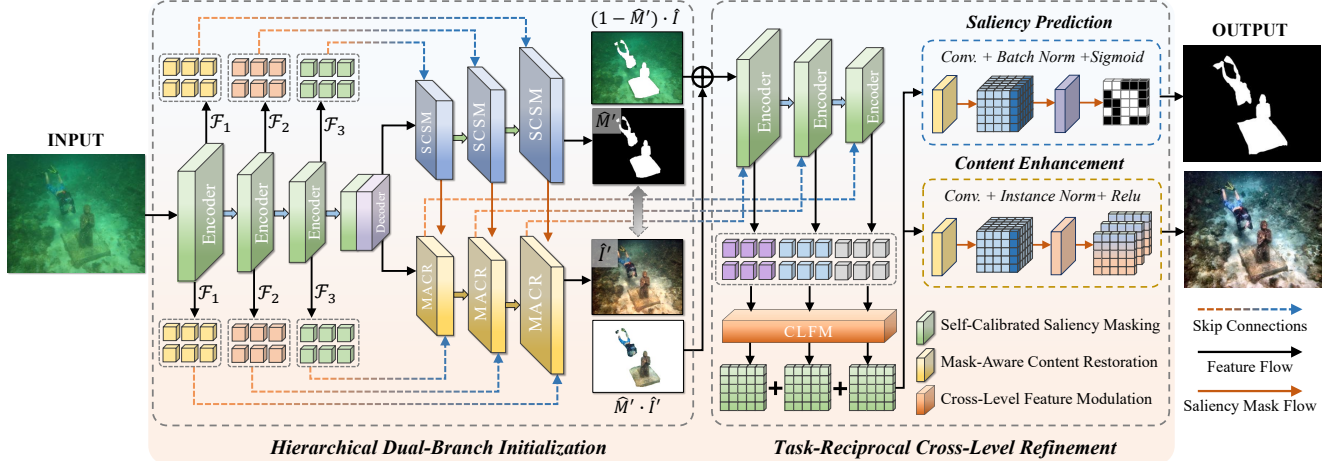


Figure 2. Overview of the proposed UniV2D. It features a semantic-driven dual-branch design, consisting of Self-Calibrated Saliency Masking (SCSM) and Mask-Aware Content Restoration (MACR) modules for initial task estimation, followed by the Cross-Level Feature Modulation (CLFM) module for joint task-reciprocal refinement of both tasks.

image features (*e.g.*, color, texture, and contour) into descriptors and then infer visual saliency by quantifying their global relative sharpness [23, 24]. Jian *et al.* [34] proposed a framework that combines the quaternionic distance-based Weber descriptor, pattern distinctness, and local contrast to highlight salient objects and suppress background regions. Instead of linearly stacking multiple convolutional layers in the network, several deep learning-based USOD methods [27, 74, 91] have incorporated visual transformers with wider receptive fields into their deep architectures. This approach helps alleviate the computational burden imposed by convolution and improves the salient object detection performance to some extent [10, 14]. However, these methods do not consider cross-level feature interactions when designing the network, which is not reliable for capturing saliency cues by improving the encoder architecture.

3. Methodology

The overall architecture of UniV2D is illustrated in Fig. 2. Diverging from conventional two-stage paradigms, UniV2D adopts a unified dual-branch design to jointly optimize underwater image restoration and salient object detection within a single network. Built upon a U-Net-like backbone [60], the framework comprises a shared hierarchical encoder and two task-specific decoder branches, enabling efficient feature reuse while mitigating task decoupling issues. The encoder extracts multi-scale features that capture both fine-grained structural details and high-level semantic context, providing a foundation for subsequent collaborative decoding.

The core of our framework lies in a two-stage optimization process: hierarchical dual-branch initialization and task-reciprocal cross-level refinement. During initializa-

tion, the saliency branch incorporates the Self-Calibrated Saliency Masking (SCSM) module to progressively localize salient regions. Simultaneously, the restoration branch employs the Mask-Aware Content Restoration (MACR) module, which leverages the predicted saliency maps as structural guidance to reconstruct clear and content-consistent images. Following this, the preliminary outputs are further enhanced through Cross-Level Feature Modulation (CLFM) modules. These modules facilitate bidirectional feature interaction across multiple scales and tasks, effectively reinforcing semantic alignment and structural fidelity. Finally, UniV2D is optimized via a joint loss function that balances saliency detection accuracy and visual restoration quality, ensuring both tasks benefit from shared supervision and mutual reinforcement.

3.1. Dual-Branch Initialization via Hierarchical Saliency Decoding

As the foundational stage of UniV2D, the Dual-Branch Initialization aims to jointly generate a coarse saliency mask and a restored image through a hierarchical decoding process. Diverging from conventional two-stage pipelines that handle saliency detection and image restoration in isolation [46, 90], our design establishes explicit task interaction at the early decoding stage, allowing the two objectives to mutually guide feature reconstruction. To this end, the decoder is organized into two parallel branches: the SCSM module produces an initial saliency prior, while the MACR module leverages these estimated cues to recover content with structural fidelity. This hierarchical architecture progressively integrates multi-scale encoder features, enabling a coarse-to-fine estimation of both tasks while maintaining intrinsic consistency.

Self-Calibrated Saliency Masking. The SCSM module

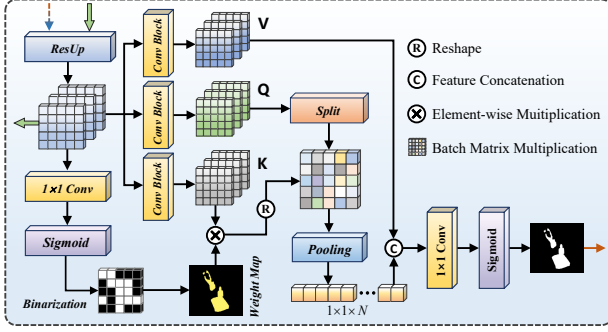


Figure 3. Architecture of the SCSM module. It employs spatial reweighting and token-guided calibration to produce an initial saliency mask from hierarchical features.

is designed to generate an adaptive saliency prior that emphasizes foreground regions while suppressing background interference. As illustrated in Fig. 3, the decoder feature \mathcal{S}_i is first fused with its corresponding skip-connected encoder feature \mathcal{F}_i via channel-wise concatenation. This is followed by a residual upsampling $\text{ResUp}(\cdot)$ to align the spatial resolution with the preceding layer:

$$\hat{X}_{in} = \text{ResUp}(\text{Cat}(\mathcal{S}_i, \mathcal{F}_i)). \quad (1)$$

Based on the fused feature \hat{X}_{in} , we estimate a coarse saliency weighting map \mathcal{M} using a 1×1 convolution to aggregate channel responses, followed by a Sigmoid activation that normalizes the output to the range $[0, 1]$. The computation is defined as:

$$\mathcal{M}_k = \sigma(\text{Conv}_{1 \times 1}(\hat{X}_{in})), \quad (2)$$

where $\sigma(\cdot)$ denotes the Sigmoid function. The resulting \mathcal{M}_k serves as a task-adaptive prior, effectively enhancing salient responses while filtering out pervasive underwater background noise.

Although \mathcal{M}_k may still contain background noise or incomplete foreground responses, it serves as a task-adaptive prior that highlights informative regions while suppressing irrelevant areas. Guided by this prior, we derive a compact global salient descriptor $\tilde{X}_k \in \mathbb{R}^C$ through attention-weighted pooling over the feature map \hat{X}_{in} , formulated as:

$$\tilde{X}_k = \frac{1}{\sum_{(i,j)} \mathcal{M}_k^{(i,j)}} \sum_{(i,j)} \mathcal{M}_k^{(i,j)} \cdot \hat{X}_{in}^{(i,j)}, \quad (3)$$

where $\mathcal{M}_k^{(i,j)}$ serves as an adaptive weight to effectively aggregate discriminative cues from salient regions.

To evaluate the semantic consistency between global salient features and local spatial features, we project both \tilde{X}_k and \hat{X}_{in} into a shared representation space using two learnable convolutional blocks ϕ_q and ϕ_k , as defined below:

$$\tilde{X}_k = \phi_k(\hat{X}_k), \quad \tilde{X}_q = \phi_q(\hat{X}_{in}), \quad (4)$$

where \tilde{X}_k and \tilde{X}_q denote the transformed feature maps within the common embedding space. $\phi_q(\cdot)$ and $\phi_k(\cdot)$ are 1×1 convolutional blocks that align the local and global representations into a comparable feature domain.

We then calculate a saliency affinity map $S \in \mathbb{R}^{1 \times H \times W}$ to quantify the semantic similarity between each pixel and the global salient region. This is achieved by concatenating \tilde{X}_k and \tilde{X}_q along the channel dimension, followed by a 1×1 convolution and non-linear activation:

$$S = \sigma\left(\text{Conv}_{1 \times 1}\left(\tanh\left(\text{Cat}(\tilde{X}_k, \tilde{X}_q)\right)\right)\right), \quad (5)$$

where $\tanh(\cdot)$ introduces non-linear feature separation to enhance the response contrast between salient and non-salient regions. The $\sigma(\cdot)$ function further maps the activation into the range $[0, 1]$, yielding a probabilistic saliency confidence map. Higher S values indicate stronger semantic relevance to the globally salient region, thereby promoting structurally consistent saliency refinement.

Following the derivation of the affinity map S , we integrate a global contextual cue \tilde{X}_v , which is obtained by projecting the fused feature \hat{X}_{in} through an additional learnable convolutional block $\phi_v(\cdot)$. The initial saliency prediction \hat{M}' is then generated by concatenating S and \tilde{X}_v , followed by a 1×1 convolution and a Sigmoid activation:

$$\hat{M}' = \sigma\left(\text{Conv}_{1 \times 1}\left(\text{Cat}(S, \tilde{X}_v)\right)\right). \quad (6)$$

This predicted mask \hat{M}' serves as an explicit structural prior for the subsequent restoration branch and is further utilized in the refinement stage to facilitate cross-task interaction. To ensure accurate foreground localization, we supervise this prediction using a binary cross-entropy loss against the ground-truth mask M_{gr} . The preliminary saliency loss is defined as:

$$\mathcal{L}_{mask}^{pre} = - \sum_{(i,j)} \left(M_{gr} \log \hat{M}'_{(i,j)} + (1 - M_{gr}) \log(1 - \hat{M}'_{(i,j)}) \right), \quad (7)$$

where $\hat{M}'_{(i,j)}$ denotes the predicted saliency at pixel (i, j) .

Mask-Aware Content Restoration. As illustrated in Fig. 4, the MACR module is designed to achieve structure-preserving restoration by leveraging the predicted saliency mask as an explicit spatial prior. Unlike previous multi-task paradigms [5] that rely on simple feature concatenation, MACR adaptively modulates restoration features to emphasize foreground structures while suppressing pervasive underwater background interference.

Given the intermediate encoder feature \mathcal{F}_i from the i -th encoder and the propagated feature \mathcal{G}_{i-1} from the previous decoding stage, MACR first aligns the spatial resolution and refines the representation through a residual upsampling and normalization block:

$$\mathcal{G}_i = \text{Cat}(\text{CNR}(\text{ResUp}(\mathcal{G}_{i-1})), \mathcal{F}_i), \quad (8)$$

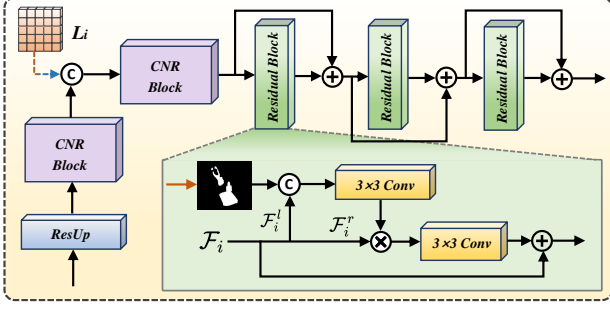


Figure 4. Architecture of the MACR module. It utilizes the predicted saliency mask as structural guidance to reconstruct restored images through mask-aware feature modulation.

where $\text{CNR}(\cdot)$ refers to a sequence of Convolution, Normalization, and ReLU activation.

To incorporate saliency-guided structural information at each level, we concatenate the decoding feature \mathcal{G}_i with the initial saliency mask \hat{M}' . We then employ a series of residual blocks to extract a saliency-aware weight map \mathcal{W}_i , which serves as a mask-modulated attention mechanism:

$$\mathcal{W}_i = \sigma \left(\text{Conv}_{3 \times 3} \left(\text{ReLU} \left(\text{Conv}_{3 \times 3} \left[\mathcal{G}_i^l; \hat{M}' \right] \right) \right) \right), \quad (9)$$

where \mathcal{G}_i^l represents the primary feature partition of \mathcal{G}_i , and $\sigma(\cdot)$ denotes the Sigmoid activation. This weight map \mathcal{W}_i effectively encapsulates the spatial importance of different regions, ensuring that the subsequent restoration process is conditioned on the semantic importance of the scene.

The generated weight map \mathcal{W}_i is employed to modulate the remaining feature partition \mathcal{G}_i^r (the right-half channels) through an attention-based residual fusion process. Specifically, \mathcal{W}_i acts as a spatial-aware modulator that is element-wise multiplied with \mathcal{G}_i^r to extract refined structural information. This modulated representation is then processed via a 3×3 convolution to produce a mask-enhanced residual \mathcal{R}_i , calculated as:

$$\mathcal{R}_i = \text{Conv}_{3 \times 3} (\mathcal{G}_i^r \odot \mathcal{W}_i), \quad (10)$$

where \odot denotes element-wise multiplication. By multiplying the feature with the weight map, the network selectively amplifies foreground textures while attenuating background clutter. To preserve the original context while incorporating these saliency-guided updates, the refined feature $\tilde{\mathcal{F}}_i$ is generated through residual aggregation and normalization:

$$\tilde{\mathcal{F}}_i = \text{ReLU}(\text{BN}(\mathcal{R}_i + \mathcal{G}_i)), \quad (11)$$

where $\text{BN}(\cdot)$ denotes Batch Normalization. This design ensures that the restoration branch remains sensitive to the semantic boundaries provided by the saliency branch, leading to more coherent and structure-aware underwater image enhancement.

3.2. Task-Reciprocal Cross-Level Refinement

Although the dual-branch initialization yields preliminary results, the restored images may still exhibit residual deficiencies such as blur, artifacts, and color distortion. Simultaneously, the initial saliency mask often suffers from incomplete object responses, which limit its effectiveness as a structural guide. To address these issues, we propose the Task-Reciprocal Cross-Level Refinement stage to achieve global semantic consistency and finer structural alignment through bidirectional task interaction.

As illustrated in Fig. 2, we first integrate the coarse restored image \hat{I}' , the initial saliency mask \hat{M}' , and the raw input I to form a saliency-aware composite \tilde{I}_{pre} . This fusion strategy explicitly reinforces content consistency by anchoring the restoration to the predicted salient regions:

$$\tilde{I}_{pre} = \hat{I}' \cdot \hat{M}' + (1 - \hat{M}') \cdot \hat{I}, \quad (12)$$

where \tilde{I}_{pre} serves as an auxiliary representation that emphasizes task-relevant regions for the subsequent refinement. This composite is then processed by a dedicated multi-scale encoder to extract deep hierarchical features, which are fused with the decoding features from the initialization stage via symmetric skip connections to preserve multi-level structural cues.

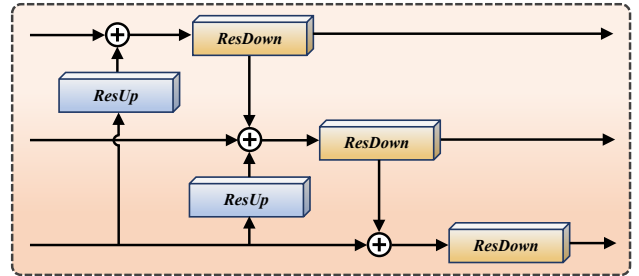


Figure 5. Architecture of the CLFM module. It facilitates bidirectional feature interaction between restoration and detection branches across multiple scales.

Cross-Level Feature Modulation. To establish effective interaction across these hierarchical representations, we introduce the Cross-Level Feature Modulation (CLFM) module, as shown in Fig. 5. Shallow features capture fine-grained textures, whereas deeper layers encode abstract semantic context. CLFM facilitates efficient cross-scale transfer by integrating task-specific cues through a series of residual-based modulation operations.

The CLFM module utilizes three pairs of residual up-sampling (ResUp) and downsampling (ResDown) paths to align spatial resolutions and adapt channel dimensions across levels. Let $\{\mathcal{F}_1, \mathcal{F}_2, \mathcal{F}_3\}$ denote the encoder features from low to high levels. We progressively modulate these features to propagate semantic and structural information as

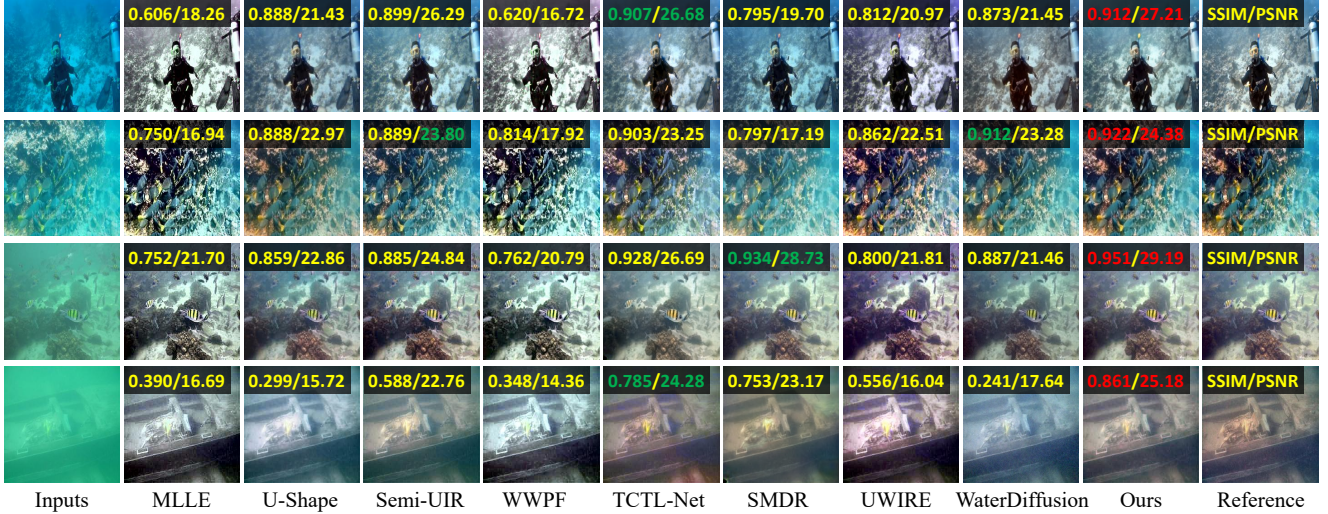


Figure 6. Qualitative comparisons between UniV2D and SOTA methods across diverse underwater degradation types (e.g., greenish, bluish, and turbid conditions). Best and second-best SSIM/PSNR scores are highlighted in red and green, respectively.

follows:

$$\mathcal{F}_1^d = \text{ResDown}(\mathcal{F}_1 + \text{ResUp}(\mathcal{F}_3)), \quad (13)$$

$$\mathcal{F}_2^d = \text{ResDown}(\mathcal{F}_1^d + \text{ResUp}(\mathcal{F}_3) + \mathcal{F}_2), \quad (14)$$

$$\mathcal{F}_3^d = \text{ResDown}(\mathcal{F}_2^d + \mathcal{F}_3), \quad (15)$$

where $\{\mathcal{F}_1^d, \mathcal{F}_2^d, \mathcal{F}_3^d\}$ represent the intermediate modulated features that encapsulate reciprocal task cues. Finally, the aggregated outputs at each level are passed to two task-specific prediction heads, yielding the high-fidelity restored image \hat{I}'' and the precise saliency mask \hat{M}'' .

3.3. Loss Function

To achieve collaborative optimization of both underwater image restoration and salient object detection, we employ a multi-task training objective that supervises the network at both the initialization and refinement stages.

Saliency Detection Loss. To supervise the final saliency map \hat{M}'' , we employ a composite loss consisting of Binary Cross-Entropy (BCE) and Intersection-over-Union (IoU) terms. While BCE ensures pixel-level classification accuracy, the IoU loss encourages global structural completeness and compensates for the imbalanced distribution of salient pixels. The refined saliency loss \mathcal{L}_{mask}^{fin} is defined as follows:

$$\mathcal{L}_{mask}^{fin} = \mathcal{L}_{BCE}(\hat{M}'', M_{gt}) + \mathcal{L}_{IoU}(\hat{M}'', M_{gt}). \quad (16)$$

Structure-Aware Reconstruction Loss. To ensure pixel-wise accuracy and structural fidelity of the restored image \hat{I}'' , we define the reconstruction loss $\mathcal{L}_{content}$ by combining the ℓ_1 norm with the Structural Similarity Index (SSIM). This combination balances local pixel intensity

consistency with global perceptual structure:

$$\mathcal{L}_{content} = \left\| \hat{I}'' - I_{gt} \right\|_1 + (1 - SSIM(\hat{I}'', I_{gt})). \quad (17)$$

Perceptual Loss. We incorporate a VGG-based perceptual loss to minimize the feature-level discrepancy between the restored image \hat{I}'' and the ground truth I_{gt} . By leveraging a pre-trained VGG-16 network [61], we ensure that the restored results align with high-level human visual perception. The perceptual loss \mathcal{L}_{vgg} is expressed as:

$$\mathcal{L}_{vgg} = \sum_{k \in \{1,2,3\}} \left\| \Phi_{vgg}^{(k)}(\hat{I}'') - \Phi_{vgg}^{(k)}(I_{gt}) \right\|_1, \quad (18)$$

where $\Phi^{(k)}_{vgg}(\cdot)$ denotes the feature activations from the k -th selected layer of the VGG-16 backbone.

Total Training Objective. The final training objective integrates the content reconstruction, perceptual similarity, and saliency prediction losses from both the initialization and refinement stages to facilitate end-to-end multi-task learning:

$$\mathcal{L}_{total} = \alpha \left(\mathcal{L}_{mask}^{pre} + \mathcal{L}_{mask}^{fin} \right) + \mathcal{L}_{content} + \mathcal{L}_{vgg}, \quad (19)$$

where \mathcal{L}_{mask}^{pre} is the initial saliency loss from the SCSM module. The hyperparameters are empirically set to $\alpha = 0.5$ to balance the convergence rates and significance of the two tasks.

4. Experiments

4.1. Experimental Setups

Implementation Details. We implement the proposed UniV2D using the PyTorch framework and conduct training

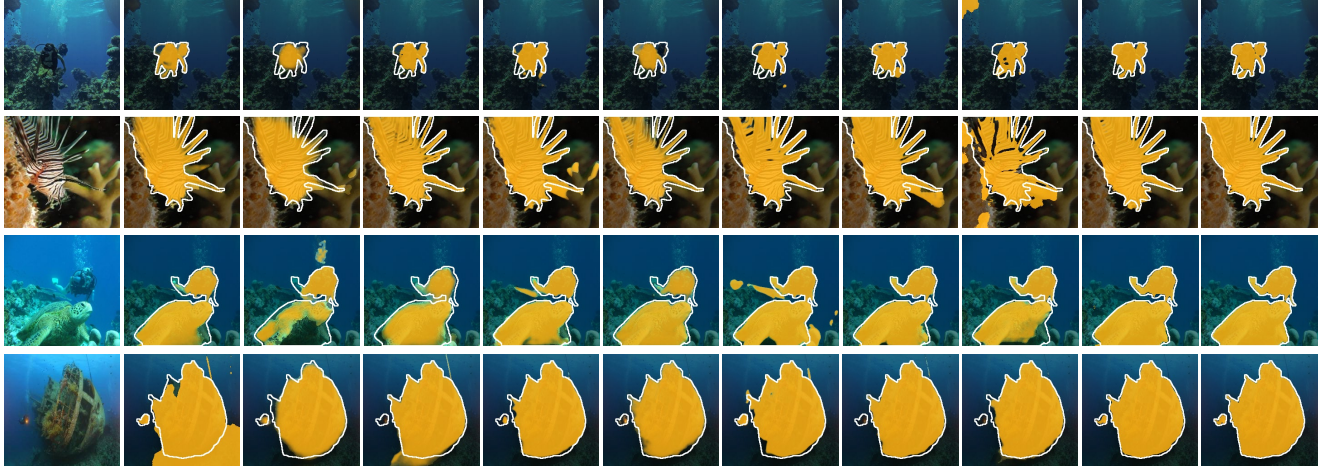


Figure 7. Qualitative comparisons between UniV2D and SOTA methods across diverse biological categories and object scales (e.g., diver, lionfish, turtle, and shipwreck). Orange regions represent predicted salient masks, while the white contours indicate ground-truth annotations.

on two NVIDIA GeForce RTX 4090 GPUs for 150 epochs. The batch size and patch size are set to 32 and 256×256 , respectively. We employ the Adam optimizer with an initial learning rate of 1×10^{-4} . Detailed hyperparameter configurations and network specifications are provided in the supplementary material to ensure reproducibility.

Benchmark Datasets. Our experiments evaluate the collaborative tasks of underwater image enhancement (UIE) and salient object detection (USOD) using several representative benchmarks. For the UIE task, we utilize UIEB [38], LSUI [53], and UWscene [32] datasets; following standard protocols, UIEB and LSUI are split into training and testing sets, with 790 and 3,779 images for training, and 100 (Test-U100) and 500 (Test-L500) images reserved for evaluation, respectively. For the USOD task, we employ USOD10K [27], USOD [33], and SUIM [31] benchmarks. All datasets consist of real-world underwater images paired with high-quality reference maps, and for those with predefined splits (e.g., UWscene and SUIM), we strictly adhere to their original configurations. To ensure a fair comparison, all baseline methods are retrained on these same datasets using their official settings to maintain benchmarking consistency.

Evaluation Metrics. For the UIE task, we adopt five widely-used metrics to assess restoration quality. These include three full-reference metrics: Structural Similarity (SSIM), Peak Signal-to-Noise Ratio (PSNR), and Perceptual Color Quality Index (PCQI), along with two no-reference metrics: UIQM [52] and UCIQE [71]. For the USOD task, we evaluate performance using four standard metrics: S-measure (S_α) [19], weighted F-measure (F_β^w) [1], max E-measure (E_ϕ^m) [18], and Mean Absolute Error (M_{AE}) [55]. These metrics collectively provide a comprehensive evaluation of both low-level visual fidelity and high-level semantic localization.

4.2. Comparison with State-of-the-Arts

We compare the proposed UniV2D model with eight state-of-the-art UIE methods, including MLE [78], U-Shape [53], Sem-UIR [30], WWPF [80], TCTL-Net [41], SMDR [76], UWIRE [6], and WaterDiffusion [5]. For salient object detection evaluation, we compare UniV2D with eight well-known USOD methods, namely U2-Net [58], MFNet [56], RMFormer [17], CATNet [64], DualSAM [77], TC-USOD [27], SPDE [35], and WaterDiffusion [5]. Notably, WaterDiffusion is the only one capable of simultaneously performing both UIE and USOD tasks within a unified framework, making it our primary baseline for multi-task evaluation.

Qualitative evaluation. Fig. 6 illustrates representative restoration results on various underwater scenes. While most approaches yield visually pleasing enhancements, the proposed UniV2D consistently achieves results that most closely align with the reference images in terms of color fidelity, content preservation, and overall contrast. Given the subjectivity of individual visual perception, we further incorporate two widely adopted quantitative image quality metrics (SSIM and PSNR) to objectively evaluate performance. The consistently higher values achieved by our UniV2D underscore its effectiveness in visual restoration tasks. Furthermore, Fig. 7 presents salient object detection results across the USOD10K, USOD, and SUIM datasets. Compared to existing techniques, UniV2D demonstrates remarkable robustness in accurately localizing salient regions and preserving fine-grained boundaries, even in challenging environments with low contrast or cluttered backgrounds.

Quantitative evaluation. The quantitative results for underwater image enhancement and salient object detection across multiple public datasets are presented in Table 1 and

Table 1. Quantitative evaluation of each UIE method on three underwater datasets: Test-U100, Test-L500, and UWscene. The best and second-best results are highlighted in **bold** and underline, respectively.

Method	Test-U100					Test-L500					UWscene				
	SSIM↑	PSNR↑	PCQI↑	UIQM↑	UCIQE↑	SSIM↑	PSNR↑	PCQI↑	UIQM↑	UCIQE↑	SSIM↑	PSNR↑	PCQI↑	UIQM↑	UCIQE↑
MLLE	0.631	16.66	0.449	4.216	0.595	0.632	19.20	0.413	4.402	0.602	0.592	14.98	0.415	4.403	0.613
U-shape	0.816	21.83	0.836	4.760	0.563	0.849	24.63	0.808	4.885	0.564	0.820	22.89	0.776	4.997	0.579
Semi-UIR	0.852	23.37	0.713	4.851	0.605	0.815	24.07	0.588	4.889	0.606	0.831	21.02	0.651	4.981	0.623
WWPF	0.711	17.58	0.511	4.504	0.603	0.680	19.42	0.434	4.634	0.609	0.648	15.80	0.428	4.641	0.627
TCTL-Net	0.906	<u>25.36</u>	0.817	4.747	0.602	0.838	22.83	0.713	4.857	0.595	0.855	23.54	0.718	4.940	0.606
SMDR	0.873	23.58	0.807	4.801	0.594	<u>0.875</u>	<u>25.22</u>	0.734	4.854	0.575	<u>0.887</u>	23.84	0.672	5.001	0.613
UWIRE	0.751	23.65	0.678	4.850	<u>0.616</u>	0.716	19.73	0.587	<u>4.948</u>	0.623	0.655	17.54	0.579	4.970	0.638
Initialization	0.860	23.76	<u>0.848</u>	4.733	0.597	0.872	24.99	<u>0.817</u>	4.856	0.576	0.861	<u>25.03</u>	<u>0.790</u>	5.006	0.572
UniV2D	<u>0.896</u>	25.85	0.852	4.913	0.619	0.888	27.31	0.828	4.957	<u>0.611</u>	0.894	26.34	0.818	5.067	<u>0.629</u>

Table 2. Quantitative evaluation of each USOD method on three underwater datasets: USOD10K, USOD, and SUIM. The best and second-best results are highlighted with **bold** and underline, respectively.

Method	USOD10K				USOD				SUIM			
	S_α ↑	F_β^w ↑	E_ϕ^m ↑	M_{AE} ↓	S_α ↑	F_β^w ↑	E_ϕ^m ↑	M_{AE} ↓	S_α ↑	F_β^w ↑	E_ϕ^m ↑	M_{AE} ↓
SUIM-Net	0.797	0.783	0.856	0.0821	0.769	0.717	0.826	0.1159	0.777	0.601	0.804	0.0957
U2-Net	0.895	0.844	0.937	0.0351	0.888	0.862	0.923	0.0541	0.816	0.718	0.899	0.0781
MFNet	0.843	0.731	0.915	0.0513	0.842	0.776	0.911	0.0758	0.781	0.642	0.820	0.0974
RMFormer	0.867	0.828	0.910	0.0439	0.880	0.876	0.912	0.0542	0.808	0.713	0.870	0.0835
CATNet	0.890	0.862	0.949	0.0299	0.878	0.865	0.925	0.0522	0.831	0.768	0.895	0.0618
DualSAM	0.916	0.909	0.959	0.0218	<u>0.906</u>	<u>0.908</u>	<u>0.940</u>	0.0397	0.853	0.804	0.909	0.0446
TC-USOD	0.912	0.905	0.953	0.0236	0.906	<u>0.896</u>	0.937	<u>0.0376</u>	0.867	0.833	<u>0.934</u>	0.0409
SPDE	<u>0.923</u>	<u>0.912</u>	<u>0.961</u>	0.0203	0.900	0.888	0.934	0.0438	<u>0.876</u>	0.863	0.926	<u>0.0382</u>
Initialization	0.894	0.867	0.947	0.0379	0.888	0.877	0.927	0.0507	0.840	0.754	0.920	0.0562
UniV2D	0.927	0.915	0.965	<u>0.0211</u>	0.912	0.901	0.946	0.0371	0.882	<u>0.858</u>	0.949	0.0351

Table 2, respectively. Our proposed UniV2D consistently achieves the best or second-best performance across nearly all metrics, particularly attaining the highest average scores in key full-reference indices. This superior performance demonstrates UniV2D’s robustness in complex underwater scenes, outperforming both task-specific SOTA models and the dual-task WaterDiffusion. These gains stem from our hierarchical dual-stage design: the SCSM and MACR modules establish robust structural priors during initialization, while the refinement stage utilizes CLFM for deep semantic alignment. This synergy facilitates mutual reinforcement, where enhanced visual features improve saliency localization, which in turn provides sharper structural guidance for final high-fidelity restoration.

4.3. Evaluation of Model Efficiency

Inference Efficiency. We first evaluate the efficiency of UniV2D by comparing its inference time with UIE and USOD methods. As illustrated in Fig. 8, we present the inference times for individual UIE and USOD tasks along the axes, while the center region represents the cumulative time of their linear cascades (*i.e.*, UIE followed by USOD). Our UniV2D achieves a remarkably low inference time of 0.016s per image, which is significantly faster than even the most efficient cascaded combination (e.g., TCTL-Net and MFNet at 0.094s). This nearly six-fold speedup validates

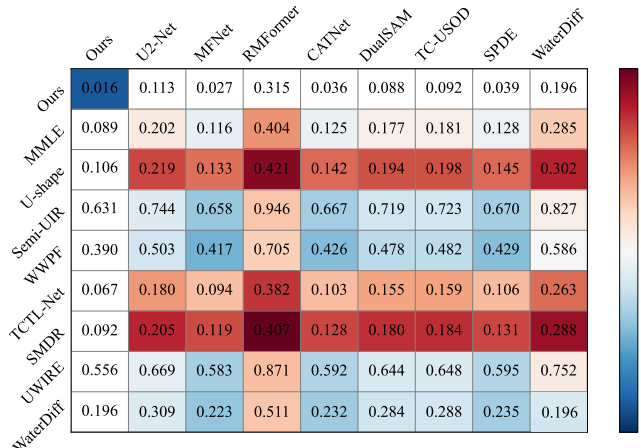


Figure 8. Efficiency evaluation of each compared method in terms of inference time. The center region indicates the summed time of two tasks at the corresponding position.

that our unified architecture effectively eliminates the redundant computational overhead inherent in conventional multi-stage pipelines.

Parameters and FLOPs. To further evaluate model complexity, we conduct a comparative analysis of parameters (M) and FLOPs (G) against deep learning-based competitors, as summarized in Table 3. Despite its dual-task ca-

Table 3. Efficiency evaluation of each compared method in terms of Parameters (M) and FLOPs (G).

UIE Methods			USOD Methods		
Config.	Params.	FLOPs	Config.	Params.	FLOPs
MLLE	<i>Null</i>	<i>Null</i>	U2-Net	44.01	37.65
U-Shape	65.60	66.20	MFNet	36.36	38.69
Semi-UIR	12.78	36.46	RMFormer	174.19	563.14
WWPF	<i>Null</i>	<i>Null</i>	CATNet	110.40	67.80
TCTL-Net	99.72	56.51	DualSAM	159.95	325.70
SMDR	12.26	46.59	TC-USOD	117.64	29.64
UWIRE	<i>Null</i>	<i>Null</i>	SPDE	115.66	41.46
WaterDiffusion	55.49	169.56	WaterDiffusion	55.49	169.56
Ours	13.29	31.23	Ours	13.29	31.23

pability, UniV2D maintains a highly compact footprint with only 13.29M parameters and 31.23G FLOPs. Notably, compared to the multi-task WaterDiffusion, UniV2D achieves a 76% reduction in parameters and an 81% decrease in computational overhead. Furthermore, UniV2D demonstrates superior efficiency even when compared to many single-task models.

4.4. Ablation Study

To verify the contribution of each core component in UniV2D, we conduct comprehensive ablation experiments focusing on the initialization and refinement stages.

Ablation Study of MACR Module. Table 4 presents the impact of the Mask-Aware Content Restoration (MACR) module across four saliency metrics. The inclusion of MACR leads to consistent improvements in S_α , F_β^w , and E_ϕ^m , alongside a significant reduction in M_{AE} . These gains demonstrate that integrating mask-aware features effectively suppresses background interference and enhances high-level semantic localization, thereby improving saliency prediction by leveraging refined visual cues.

Table 4. Quantitative ablation of the MACR module.

-w/o MACR	-w/ MACR	$S_\alpha \uparrow$	$F_\beta^w \uparrow$	$E_\phi^m \uparrow$	$M_{AE} \downarrow$
✓		0.888	0.859	0.941	0.0421
	✓	0.925	0.910	0.963	0.0217

Ablation Study of SCSM Module. Table 5 summarizes the performance contribution of the self-calibrated saliency masking (SCSM) module to the visual restoration task. The introduction of SCSM yields superior SSIM, PSNR, UIQM, and UCIQE scores, validating its effectiveness in optimizing perceived contrast and color constancy. These results indicate that by providing fine-grained saliency-guided attention, the module enables the network to adaptively concentrate on informative regions, resulting in higher restoration fidelity and overall visual quality.

Visual ablation of MACR and SCSM. Fig. 9 provides a qualitative comparison to illustrate the structural contributions of both modules. Specifically, the MACR module en-

Table 5. Quantitative ablation of the SCSM module.

-w/o SCSM	-w/ SCSM	SSIM \uparrow	PSNR \uparrow	UIQM \uparrow	UCIQE \uparrow
✓		0.863	24.979	4.969	0.574
	✓	0.893	26.492	5.031	0.623

hances the regional completeness and boundary sharpness of the predicted saliency masks. The SCSM module effectively mitigates underwater color casts and improves structural clarity in the restored images. These visual outcomes further confirm the effectiveness of the dual-branch interaction in fostering task-specific enhancements.

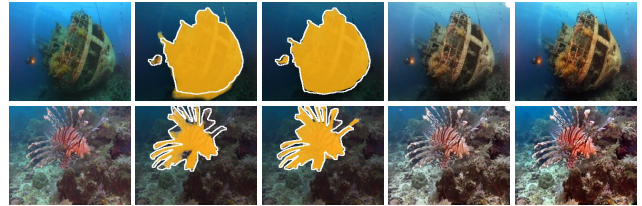


Figure 9. Visual ablation of the SCSM and MACR modules.

Effectiveness of Saliency Mask Flow. Table 6 evaluates the effectiveness of the Saliency Mask Flow (SMF) during both the initialization and refinement stages. In both phases, the incorporation of SMF consistently optimizes all saliency metrics, yielding higher S_α , F_β^w , and E_ϕ^m scores alongside a diminished M_{AE} . Notably, the more significant performance leap in the refinement stage suggests that SMF effectively propagates semantic cues across stages, thereby enforcing saliency consistency and contributing to more robust and accurate object localization.

Table 6. Effectiveness of Saliency Mask Flow (SMF) across initialization and refinement stages.

	Config.	$S_\alpha \uparrow$	$F_\beta^w \uparrow$	$E_\phi^m \uparrow$	$M_{AE} \downarrow$
Initialization	-w/o SMF	0.879	0.838	0.928	0.0365
	-w/ SMF	0.894	0.867	0.947	0.0319
Refinement	-w/o SMF	0.885	0.853	0.939	0.0340
	-w/ SMF	0.925	0.910	0.963	0.0217

5. Conclusion

This paper presents UniV2D, a novel unified framework designed for the joint optimization of USOD and UIE. Diverging from conventional cascaded or multi-stage baselines, UniV2D integrates both tasks within a single, cohesive network, enabling low-level enhancement and high-level perception to mutually reinforce each other. Specifically, the proposed hierarchical dual-branch initialization utilizes the SCSM module to estimate robust saliency priors, while the MACR module restores visual content under the explicit

guidance of these predicted masks. Subsequently, a task-reciprocal refinement stage employs the CLFM module to enforce deep semantic alignment and preserve fine-grained structural details across multiple scales. Extensive experiments on several benchmarks demonstrate that UniV2D consistently achieves state-of-the-art performance in both UIE and USOD tasks.

References

- [1] Radhakrishna Achanta, Sheila Hemami, Francisco Estrada, and Sabine Susstrunk. Frequency-tuned salient region detection. In *Proceedings of the IEEE/CVF Conference on Computer Vision and Pattern Recognition*, pages 1597–1604, 2009. 7
- [2] Hengyue Bi, Long Chen, Jingchao Cao, Jingyang Wang, Jinghao Sun, Yuan Rao, and Junyu Dong. Seadiff: Underwater image enhancement with degradation-aware diffusion model. *IEEE Transactions on Circuits and Systems for Video Technology*, 35(12):12212–12226, 2025. 2
- [3] Jingchao Cao, Wangzhen Peng, Yutao Liu, Junyu Dong, Patrick Le Callet, and Sam Kwong. Erd: Encoder-residual-decoder neural network for underwater image enhancement. *IEEE Transactions on Circuits and Systems for Video Technology*, 35(9):8958–8972, 2025. 2
- [4] Laibin Chang, Huajun Song, Mingjie Li, and Ming Xiang. Uidef: A real-world underwater image dataset and a color-contrast complementary image enhancement framework. *ISPRS Journal of Photogrammetry and Remote Sensing*, 196: 415–428, 2023. 1
- [5] Laibin Chang, Yunke Wang, Longxiang Deng, Bo Du, and Chang Xu. Waterdiffusion: Learning a prior-involved unrolling diffusion for joint underwater saliency detection and visual restoration. In *Proceedings of the AAAI Conference on Artificial Intelligence*, pages 1998–2006, 2025. 2, 4, 7
- [6] Laibin Chang, Yunke Wang, Bo Du, and Chang Xu. Rectangling and enhancing underwater stitched image via content-aware warping and perception balancing. *Neural Networks*, 181:106809, 2025. 7
- [7] Laibin Chang, Yunke Wang, JiaXing Huang, Longxiang Deng, Bo Du, and Chang Xu. Marine saliency segmenter: Object-focused conditional diffusion with region-level semantic knowledge distillation. *arXiv preprint arXiv:2504.02391*, 2025. 2
- [8] Laibin Chang, Yunke Wang, Bo Du, and Chang Xu. Color correction meets cross-spectral refinement: a distribution-aware diffusion for underwater image restoration. *IEEE Transactions on Multimedia*, 2026. 2
- [9] Long Chen, Zheheng Jiang, Lei Tong, Zhihua Liu, Aite Zhao, Qianni Zhang, Junyu Dong, and Huiyu Zhou. Perceptual underwater image enhancement with deep learning and physical priors. *IEEE Transactions on Circuits and Systems for Video Technology*, 31(8):3078–3092, 2020. 2
- [10] Long Chen, Haohan Yu, Xirui Dong, Yaxin Li, Jialie Shen, Jiangrong Shen, and Qi Xu. Bauodnet for class imbalance learning in underwater object detection. *IEEE Transactions on Emerging Topics in Computational Intelligence*, 9(3):2452–2461, 2024. 3
- [11] Yuehan Chen, Jiqing Zhang, Yafeng Li, Yudong Li, Haoming Tang, Huibing Wang, and Xianping Fu. Fusion-based channel-wise isotropic convergent real-time underwater image enhancement. *IEEE Transactions on Circuits and Systems for Video Technology*, 35(10):9763–9774, 2025. 2
- [12] Runmin Cong, Hongyu Liu, Chen Zhang, Wei Zhang, Feng Zheng, Ran Song, and Sam Kwong. Point-aware interaction and cnn-induced refinement network for rgb-d salient object detection. In *Proceedings of the 31st ACM international conference on multimedia*, pages 406–416, 2023. 1
- [13] Runmin Cong, Ning Yang, Hongyu Liu, Dingwen Zhang, Qingming Huang, Sam Kwong, and Wei Zhang. Trnet: Two-tier recursion network for co-salient object detection. *IEEE Transactions on Circuits and Systems for Video Technology*, 35(6):5844–5857, 2025. 1
- [14] Runmin Cong, Zongji Yu, Hao Fang, Haoyan Sun, and Sam Kwong. Uis-mamba: exploring mamba for underwater instance segmentation via dynamic tree scan and hidden state weaken. In *Proceedings of the 33rd ACM International Conference on Multimedia*, pages 343–352, 2025. 3
- [15] Runmin Cong, Zhiyang Chen, Hao Fang, Sam Kwong, and Wei Zhang. Breaking barriers, localizing saliency: A large-scale benchmark and baseline for condition-constrained salient object detection. *IEEE Transactions on Pattern Analysis and Machine Intelligence*, 48(4):4167–4183, 2026. 1
- [16] Longxiang Deng, Laibin Chang, and Wei Liu. Frequency-driven diffusion: A hierarchical attention weighting framework for underwater image restoration. *Computational Intelligence*, 41(4):e70095, 2025. 2
- [17] Xinhao Deng, Pingping Zhang, Wei Liu, and Huchuan Lu. Recurrent multi-scale transformer for high-resolution salient object detection. In *Proceedings of the 31st ACM International Conference on Multimedia*, pages 7413–7423, 2023. 2, 7
- [18] Dengping Fan, Cheng Gong, Yang Cao, Bo Ren, Mingming Cheng, and Ali Borji. Enhanced-alignment measure for binary foreground map evaluation. *arXiv:1805.10421*, 2018. 7
- [19] Deng-Ping Fan, Ming-Ming Cheng, Yun Liu, Tao Li, and Ali Borji. Structure-measure: A new way to evaluate foreground maps. In *Proceedings of the IEEE/CVF International Conference on Computer Vision*, pages 4548–4557, 2017. 7
- [20] Guodong Fan, Shengning Zhou, Zhen Hua, Jinjiang Li, and Jingchun Zhou. Llava-based semantic feature modulation diffusion model for underwater image enhancement. *Information Fusion*, page 103566, 2025. 2
- [21] Shixuan Gao, Pingping Zhang, Tianyu Yan, and Huchuan Lu. Multi-scale and detail-enhanced segment anything model for salient object detection. In *Proceedings of the 32nd ACM International Conference on Multimedia*, pages 9894–9903, 2024. 1
- [22] Chao Hao, Zitong Yu, Xin Liu, Jun Xu, Huanjing Yue, and Jingyu Yang. A simple yet effective network based on vision transformer for camouflaged object and salient object detection. *IEEE Transactions on Image Processing*, 34:608–622, 2025. 1
- [23] Xiao He, Chang Tang, Xinwang Liu, Wei Zhang, Kun Sun, and Jiangfeng Xu. Object detection in hyperspectral image

- via unified spectral–spatial feature aggregation. *IEEE Transactions on Geoscience and Remote Sensing*, 61:1–13, 2023. 3
- [24] Xiao He, Chang Tang, Xin Zou, and Wei Zhang. Multispectral object detection via cross-modal conflict-aware learning. In *Proceedings of the 31st ACM International Conference on Multimedia*, pages 1465–1474, 2023. 3
- [25] Lin Hong, Xin Wang, De-Sheng Zhang, Ming Zhao, and Hang Xu. Vision-based underwater inspection with portable autonomous underwater vehicle: Development, control, and evaluation. *IEEE Transactions on Intelligent Vehicles*, 9(1): 2197–2209, 2024. 2
- [26] Lin Hong, Xin Wang, Yihao Li, and Xia Wang. Usis16k: high-quality dataset for underwater salient instance segmentation. *arXiv preprint arXiv:2506.19472*, 2025. 2
- [27] Lin Hong, Xin Wang, Gan Zhang, and Ming Zhao. Usod10k: a new benchmark dataset for underwater salient object detection. *IEEE Transactions on Image Processing*, 34:1602–1615, 2025. 2, 3, 7
- [28] Xihang Hu, Fuming Sun, Jing Sun, Fasheng Wang, and Haojie Li. Cross-modal fusion and progressive decoding network for rgb-d salient object detection. *International Journal of Computer Vision*, 132(8):3067–3085, 2024. 1
- [29] Dongmei Huang, Yan Wang, Wei Song, Jean Sequeira, and Sébastien Mavromatis. Shallow-water image enhancement using relative global histogram stretching based on adaptive parameter acquisition. In *2018 International Conference on MultiMedia Modeling*, pages 453–465, 2018. 2
- [30] Shirui Huang, Keyan Wang, Huan Liu, Jun Chen, and Yunsong Li. Contrastive semi-supervised learning for underwater image restoration via reliable bank. In *Proceedings of the IEEE/CVF Conference on Computer Vision and Pattern Recognition*, pages 18145–18155, 2023. 2, 7
- [31] Md Jahidul Islam, Chelsey Edge, Yuyang Xiao, Peigen Luo, Muntaqim Mehtaz, Christopher Morse, Sadman Sakib Enan, and Junaed Sattar. Semantic segmentation of underwater imagery: Dataset and benchmark. In *2020 IEEE/RSJ International Conference on Intelligent Robots and Systems*, pages 1769–1776, 2020. 7
- [32] Md Jahidul Islam, Youya Xia, and Junaed Sattar. Fast underwater image enhancement for improved visual perception. *IEEE Robotics and Automation Letters*, 5(2):3227–3234, 2020. 7
- [33] Md Jahidul Islam, Ruobing Wang, and Junaed Sattar. Svam: Saliency-guided visual attention modeling by autonomous underwater robots. *arXiv:2011.06252*, 2021. 7
- [34] Muwei Jian, Qiang Qi, Junyu Dong, Yilong Yin, and Kin-Man Lam. Integrating qdwd with pattern distinctness and local contrast for underwater saliency detection. *Journal of Visual Communication and Image Representation*, 53:31–41, 2018. 3
- [35] Jianhui Jin, Qiuping Jiang, Qingyuan Wu, Binwei Xu, and Runmin Cong. Underwater salient object detection via dual-stage self-paced learning and depth emphasis. *IEEE Transactions on Circuits and Systems for Video Technology*, 35(3): 2147–2160, 2025. 2, 7
- [36] Maria Kanwal, M Mohsin Riaz, and Abdul Ghafoor. Unveiling underwater structures: pyramid saliency detection via homomorphic filtering. *Multimedia Tools and Applications*, pages 1–18, 2024. 2
- [37] Nitin Kumar, Harish Kumar Sardana, and SN Shome. Saliency based shape extraction of objects in unconstrained underwater environment. *Multimedia Tools and Applications*, 78:15121–15139, 2019. 2
- [38] Chongyi Li, Chunle Guo, Wenqi Ren, Runmin Cong, Junhui Hou, Sam Kwong, and Dacheng Tao. An underwater image enhancement benchmark dataset and beyond. *IEEE Transactions on Image Processing*, 29:4376–4389, 2020. 7
- [39] Hua Li, Shijie Lian, Zhiyuan Li, Runmin Cong, and Sam Kwong. Uwsam: Segment anything model guided underwater instance segmentation and a large-scale benchmark dataset. *arXiv e-prints*, pages arXiv–2505, 2025. 2
- [40] Hua Li, Gaowei Lin, Zhiyuan Li, Sam Kwong, and Runmin Cong. Fscdiff: Frequency-spatial entangled conditional diffusion model for underwater salient object detection. In *Proceedings of the 33rd ACM International Conference on Multimedia*, pages 8379–8388, 2025. 1
- [41] Kunqian Li, Hongtao Fan, Qi Qi, Chi Yan, Kun Sun, and QM Jonathan Wu. Tctl-net: Template-free color transfer learning for self-attention driven underwater image enhancement. *IEEE Transactions on Circuits and Systems for Video Technology*, 34(6):4682–4697, 2024. 7
- [42] Shaoming Li, Ziyi Wang, Rong Dai, Yaqing Wang, Fangxun Zhong, and Yunhui Liu. Efficient underwater object detection with enhanced feature extraction and fusion. *IEEE Transactions on Industrial Informatics*, 21(6):4904–4914, 2025. 1
- [43] Shijie Lian, Hua Li, Runmin Cong, Suqi Li, Wei Zhang, and Sam Kwong. Watermark: Instance segmentation for underwater imagery. In *Proceedings of the IEEE/CVF International Conference on Computer Vision*, pages 1305–1315, 2023. 2
- [44] Shijie Lian, Ziyi Zhang, Hua Li, Wenjie Li, Laurence Tianruo Yang, Sam Kwong, and Runmin Cong. Diving into underwater: Segment anything model guided underwater salient instance segmentation and a large-scale dataset. *arXiv preprint arXiv:2406.06039*, 2024. 2
- [45] Jia Lin, Xiaofei Zhou, Jiyuan Liu, Runmin Cong, Guodao Zhang, Zhi Liu, and Jiyong Zhang. Sam-daq: Segment anything model with depth-guided adaptive queries for rgb-d video salient object detection. In *Proceedings of the AAAI Conference on Artificial Intelligence*, pages 6952–6960, 2026. 1
- [46] Risheng Liu, Zhiying Jiang, Shuzhou Yang, and Xin Fan. Twin adversarial contrastive learning for underwater image enhancement and beyond. *IEEE Transactions on Image Processing*, 31:4922–4936, 2022. 2, 3
- [47] Tingwei Liu, Runyu Wang, Miao Zhang, Yongri Piao, and Huchuan Lu. Auto-usod: searching topology for underwater salient object detection. In *Chinese Conference on Pattern Recognition and Computer Vision (PRCV)*, pages 3–16, 2024. 2
- [48] Yi Liu, Qiuping Jiang, Xingbo Li, Ting Luo, and Wenqi Ren. Toward better than pseudo-reference in underwater image enhancement. *IEEE Transactions on Image Processing*, 34: 6168–6179, 2025. 2

- [49] Yiwen Liu, Xiaoyu Zhang, Jinchao Zhu, Biting Ma, Yutai Duan, and Panlong Tan. Hdanet: Enhancing underwater salient object detection with physics-inspired multimodal joint learning. *IEEE Transactions on Geoscience and Remote Sensing*, 63:1–14, 2025. 2
- [50] Siqi Lu, Fengxu Guan, Hanyu Zhang, and Haitao Lai. Underwater image enhancement method based on denoising diffusion probabilistic model. *Journal of Visual Communication and Image Representation*, 96:103926, 2023. 2
- [51] Qianwen Ma, Xiaobo Li, Bincheng Li, Zhen Zhu, Jing Wu, Feng Huang, and Haofeng Hu. Stamf: Synergistic transformer and mamba fusion network for rgb-polarization based underwater salient object detection. *Information Fusion*, 122:103182, 2025. 1
- [52] Karen Panetta, Chen Gao, and Sos Agaian. Human-visual-system-inspired underwater image quality measures. *IEEE Journal of Oceanic Engineering*, 41(3):541–551, 2016. 7
- [53] Lintao Peng, Chunli Zhu, and Liheng Bian. U-shape transformer for underwater image enhancement. *IEEE Transactions on Image Processing*, 32:3066–3079, 2023. 7
- [54] Yan-Tsung Peng, Yu-Cheng Lin, Wen-Yi Peng, and Chen-Yu Liu. Blurriness-guided underwater salient object detection and data augmentation. *IEEE Journal of Oceanic Engineering*, 49(3):1089–1103, 2024. 2
- [55] Federico Perazzi, Philipp Krähenbühl, Yael Pritch, and Alexander Hornung. Saliency filters: Contrast based filtering for salient region detection. In *Proceedings of the IEEE/CVF Conference on Computer Vision and Pattern Recognition*, pages 733–740, 2012. 7
- [56] Yongri Piao, Jian Wang, Miao Zhang, and Huchuan Lu. Mfnet: Multi-filter directive network for weakly supervised salient object detection. In *Proceedings of the IEEE/CVF International Conference on Computer Vision*, pages 4136–4145, 2021. 7
- [57] Qi Qi, Yongchang Zhang, Fei Tian, QM Jonathan Wu, Kunqian Li, Xin Luan, and Dalei Song. Underwater image co-enhancement with correlation feature matching and joint learning. *IEEE Transactions on Circuits and Systems for Video Technology*, 32(3):1133–1147, 2022. 2
- [58] Xuebin Qin, Zichen Zhang, Chenyang Huang, Masood Dehghan, Osmar R Zaiane, and Martin Jagersand. U2-net: Going deeper with nested u-structure for salient object detection. *Pattern Recognition*, 106:107404, 2020. 7
- [59] Yuhao Qing, Si Liu, Hai Wang, and Yueying Wang. Dif-fuie: Learning latent global priors in diffusion models for underwater image enhancement. *IEEE Transactions on Multimedia*, pages 1–14, 2024. 2
- [60] Olaf Ronneberger, Philipp Fischer, and Thomas Brox. U-net: Convolutional networks for biomedical image segmentation. In *International Conference on Medical Image Computing and Computer-Assisted Intervention*, pages 234–241, 2015. 3
- [61] Karen Simonyan and Andrew Zisserman. Very deep convolutional networks for large-scale image recognition. *arXiv preprint arXiv:1409.1556*, 2014. 6
- [62] Huajun Song, Laibin Chang, Ziwei Chen, and Peng Ren. Enhancement-registration-homogenization (erh): A comprehensive underwater visual reconstruction paradigm. *IEEE Transactions on Pattern Analysis and Machine Intelligence*, 44(10):6953–6967, 2022. 2
- [63] Huajun Song, Laibin Chang, Hao Wang, and Peng Ren. Dual-model: Revised imaging network and visual perception correction for underwater image enhancement. *Engineering Applications of Artificial Intelligence*, 125:106731, 2023. 2
- [64] Fuming Sun, Peng Ren, Bowen Yin, Fasheng Wang, and Haojie Li. Catnet: A cascaded and aggregated transformer network for rgb-d salient object detection. *IEEE Transactions on Multimedia*, 26:2249–2262, 2023. 7
- [65] Hao Tang, Zechao Li, Dong Zhang, Shengfeng He, and Jinhui Tang. Divide-and-conquer: Confluent triple-flow network for rgb-t salient object detection. *IEEE Transactions on Pattern Analysis and Machine Intelligence*, 47(3):1958–1974, 2024. 1
- [66] Hao Wang, Shixin Sun, Laibin Chang, Huanyu Li, Wenwen Zhang, Alejandro C Frery, and Peng Ren. Inspiration: A reinforcement learning-based human visual perception-driven image enhancement paradigm for underwater scenes. *Engineering Applications of Artificial Intelligence*, 133:108411, 2024. 2
- [67] Yi Wang, Ruili Wang, Xin Fan, Tianzhu Wang, and Xi-angjian He. Pixels, regions, and objects: Multiple enhancement for salient object detection. In *Proceedings of the IEEE/CVF Conference on Computer Vision and Pattern Recognition*, pages 10031–10040, 2023. 1
- [68] Zhengyong Wang, Liquan Shen, Mai Xu, Mei Yu, Kun Wang, and Yufei Lin. Domain adaptation for underwater image enhancement. *IEEE Transactions on Image Processing*, 32:1442–1457, 2023. 2
- [69] Huiyang Wu, Qiuping Jiang, Zongwei Wu, Runmin Cong, Cédric Demonceaux, Yi Yang, and Xiangyang Ji. High-resolution underwater creature segmentation. *IEEE Transactions on Image Processing*, 34:7759–7772, 2025. 2
- [70] Qingyao Wu, Zhenqi Fu, Hong Lin, Chenyu Ma, Xiaotong Tu, and Xinghao Ding. Effiseanet: Pioneering lightweight network for underwater salient object detection. In *Proceedings of the Asian Conference on Computer Vision*, pages 1486–1501, 2024. 2
- [71] Miao Yang and Arcot Sowmya. An underwater color image quality evaluation metric. *IEEE Transactions on Image Processing*, 24(12):6062–6071, 2015. 7
- [72] Shudi Yang, Xing Cui, Sen Zhu, Senqi Tan, Jiaxiong Wu, and Fu Chang. Saliency detection of turbid underwater images based on depth attention adversarial network. In *International Conference on Autonomous Unmanned Systems*, pages 154–163, 2023. 2
- [73] Genji Yuan, Jintao Song, and Jinjiang Li. If-usod: Multimodal information fusion interactive feature enhancement architecture for underwater salient object detection. *Information Fusion*, 117:102806, 2025. 2
- [74] Mingfeng Zha, Guoqing Wang, Yunqiang Pei, Tianyu Li, Xiongxin Tang, Chongyi Li, Yang Yang, and Heng Tao Shen. Heterogeneous experts and hierarchical perception for underwater salient object detection. *IEEE Transactions on Image Processing*, 34:3703–3717, 2025. 2, 3

- [75] Chen Zhang, Runmin Cong, Qinwei Lin, Lin Ma, Feng Li, Yao Zhao, and Sam Kwong. Cross-modality discrepant interaction network for rgb-d salient object detection. In *Proceedings of the 29th ACM international conference on multimedia*, pages 2094–2102, 2021. 1
- [76] Dehuan Zhang, Jingchun Zhou, Chunle Guo, Weishi Zhang, and Chongyi Li. Synergistic multiscale detail refinement via intrinsic supervision for underwater image enhancement. In *Proceedings of the AAAI Conference on Artificial Intelligence*, pages 7033–7041, 2024. 7
- [77] Pingping Zhang, Tianyu Yan, Yang Liu, and Huchuan Lu. Fantastic animals and where to find them: segment any marine animal with dual sam. In *Proceedings of the IEEE/CVF Conference on Computer Vision and Pattern Recognition*, pages 2578–2587, 2024. 7
- [78] Weidong Zhang, Peixian Zhuang, Hai-Han Sun, Guohou Li, Sam Kwong, and Chongyi Li. Underwater image enhancement via minimal color loss and locally adaptive contrast enhancement. *IEEE Transactions on Image Processing*, 31:3997–4010, 2022. 7
- [79] Weidong Zhang, Qingmin Liu, Yikun Feng, Lei Cai, and Peixian Zhuang. Underwater image enhancement via principal component fusion of foreground and background. *IEEE Transactions on Circuits and Systems for Video Technology*, 34(11):10930–10943, 2024. 2
- [80] Weidong Zhang, Ling Zhou, Peixian Zhuang, Guohou Li, Xipeng Pan, Wenyi Zhao, and Chongyi Li. Underwater image enhancement via weighted wavelet visual perception fusion. *IEEE Transactions on Circuits and Systems for Video Technology*, 34(4):2469–2483, 2024. 7
- [81] Xu Zhang, Huan Zhang, Guoli Wang, Qian Zhang, Lefei Zhang, and Bo Du. Uniuir: Considering underwater image restoration as an all-in-one learner. *IEEE Transactions on Image Processing*, 34:6963–6977, 2025. 2
- [82] Xu Zhang, Huan Zhang, Guoli Wang, Qian Zhang, Lefei Zhang, and Bo Du. Uniuir: Considering underwater image restoration as an all-in-one learner. *arXiv preprint arXiv:2501.12981*, 2025. 2
- [83] Xu Zhang, Jiaqi Ma, Guoli Wang, Qian Zhang, Huan Zhang, and Lefei Zhang. Perceive-ir: Learning to perceive degradation better for all-in-one image restoration. *IEEE Transactions on Image Processing*, 35:2018–2033, 2026. 1
- [84] Xu Zhang, Huan Zhang, Guoli Wang, Qian Zhang, and Lefei Zhang. Clearair: A human-visual-perception-inspired all-in-one image restoration. In *Proceedings of the AAAI Conference on Artificial Intelligence*, pages 12861–12869, 2026. 2
- [85] Yuhan Zhang, Jieyu Yuan, and Zhanchuan Cai. Dcgf: Diffusion-color guided framework for underwater image enhancement. *IEEE Transactions on Geoscience and Remote Sensing*, 63:1–12, 2025. 2
- [86] Zengxi Zhang, Zhiying Jiang, Long Ma, Jinyuan Liu, Xin Fan, and Risheng Liu. Hupe: Heuristic underwater perceptual enhancement with semantic collaborative learning. *International Journal of Computer Vision*, pages 1–19, 2025. 2
- [87] Chen Zhao, Weiling Cai, Chenyu Dong, and Chengwei Hu. Wavelet-based fourier information interaction with frequency diffusion adjustment for underwater image restoration. In *Proceedings of the IEEE/CVF Conference on Computer Vision and Pattern Recognition*, pages 8281–8291, 2024. 2
- [88] Ziqiang Zheng, Yiwei Chen, Huimin Zeng, Tuan-Anh Vu, Binh-Son Hua, and Sai-Kit Yeung. Marineinst: A foundation model for marine image analysis with instance visual description. In *European Conference on Computer Vision*, pages 239–257, 2024. 2
- [89] Jingchun Zhou, Shiyin Wang, Zifan Lin, Qiuping Jiang, and Ferdous Sohel. A pixel distribution remapping and multi-prior retinex variational model for underwater image enhancement. *IEEE Transactions on Multimedia*, 26:7838–7849, 2024. 2
- [90] Jingchun Zhou, Zongxin He, Dehuan Zhang, Siyuan Liu, Xianning Fu, and Xuelong Li. Spatial residual for underwater object detection. *IEEE Transactions on Pattern Analysis and Machine Intelligence*, 47(6):4996–5013, 2025. 3
- [91] Wujie Zhou, Beibei Tang, Runmin Cong, and Qiuping Jiang. Turbidity-similarity decoupling: Feature-consistent mutual learning for underwater salient object detection. *IEEE Transactions on Image Processing*, 35:495–510, 2026. 3
- [92] Wujie Zhou, Beibei Tang, Xiena Dong, and Fangfang Qiang. Prompt then refine: Prompt-free sam-enhanced collaborative learning network for detecting salient objects in underwater images. *IEEE Transactions on Neural Networks and Learning Systems*, pages 1–15, 2026. 2
- [93] Jifeng Zhu, Wenyu Cai, Meiyang Zhang, Yuxin Lin, and Mingming Liu. Saliency detection for underwater moving object with sonar based on motion estimation and multi-trajectory analysis. *Pattern Recognition*, 158:111043, 2025. 2
- [94] Jiayi Zhu, Xuebin Qin, and Abdulmotaleb El Saddik. Dcnet: Divide-and-conquer for salient object detection. *Pattern Recognition*, 157:110903, 2025. 1
- [95] Linwei Zhu, Junhao Zhu, Xu Zhang, Huan Zhang, Ye Li, Runmin Cong, and Sam Kwong. Enhanced quality aware scalable underwater image compression. *ACM Transactions on Multimedia Computing, Communications and Applications*, 2026. 2
- [96] Peixian Zhuang, Jiamin Wu, Fatih Porikli, and Chongyi Li. Underwater image enhancement with hyper-laplacian reflectance priors. *IEEE Transactions on Image Processing*, 31:5442–5455, 2022. 2